Modeling of isothermal stress cycling degradation of shape memory alloys using non-constant material parameters

Xiaoyong ZHANG[1,*], Xiaojun YAN[2], Huimin XIE[1]

[1] AML, School of Aerospace, Tsinghua University, Beijing, 100084, China.
[2] School of Energy and Power Engineering, Beihang University, Beijing 100191, China.
* Corresponding author: zhangyong9119@163.com

Abstract Experimental investigations on superelastic shape memory alloy (SMA) wires subjected to isothermal stress cycling show significant performance degradations, including the accumulation of the plastic strain, the reduction of the maximum transformation strain and the evolution of the transformation temperatures. The cyclic degradation of SMAs must be carefully studied and understood when the alloys are used in the SMA based actuators and vibration isolators. Motivated by these issues, the present work aims to develop a comprehensive approach for the cyclic behavior of SMAs taking into account degradations caused by isothermal stress cycling in the superelastic regime. The new cyclic constitutive model is constructed based on the thermodynamic frame proposed by Boyd and Lagoudas, and evolution laws for the plastic strain as well as non-constant material parameters including the maximum transformation strain and four transformation temperatures are also constructed. Finally, numerical simulations based on the proposed constitutive model are also performed in our work, and good correlations are observed.

Keywords Shape Memory Alloys, Cyclic Degradation, Constitutive Model, Non-constant Material Parameters

1. Introduction

Shape memory alloys (SMAs) exhibit many special properties due to their thermo-elastic martensite transformation, such as shape memory effect, superelasticity (or pseudoelasticity) and damping [1]. Among these thermal-mechanical behaviors, superelasticity is particularly interesting. Superelastic behavior is revealed when the SMA material is mechanically loading under a surrounding temperature higher than the austenite finish temperature. After unloading, SMA material can recover its initial shape and the stress–strain response shows a typical hysteretic loop. This unique superelasticity promotes SMAs to be used in medical applications, such as arterial stents, medical guidewires and catheters [2]. Also, the typical hysteretic loop in the stress–strain space reveals that SMA is a kind of energy dissipation material. Taken the advantage of this property, SMAs are also used in vibration isolation applications, such as seismic isolation and mechanical vibration isolation.

Motivated by these applications, many constitutive models were developed to simulate the thermal-mechanical behavior of SMAs in the superelastic regime over the last thirty years [3-10]. However, among these investigations, very few studies consider the performance degradation of SMAs under isothermal stress cycling, which is more pertinent when SMAs are used in vibration isolation applications [11-15]. Until recently, Kan and Kang introduced the cumulated martensite volume fraction as an internal variable to account for the evolution of residual induced martensite and transformation induced plastic strain during stress-controlled cyclic loading [16]. Zaki and Moumni used internal stress, residual strain and cumulated martensite volume fraction as internal variables to simulate the behavior of SMA in the case of cyclic superelasticity [17]. Saint-Sulpice et al. introduced the residual martensite volume fraction to account for the evolution of residual strain and transformation surface during isothermal stress cyclic loading [18].

The aforementioned models usually consider the plastic strain accumulation and/or the transformation surface evolution (which is associated with the evolution of maximum

transformation strain). However, the transformation temperatures of the alloy were demonstrated to change as a function of the thermal/stress cycling number [19-21]. Moreover, the evolution of transformation temperatures can significantly affect the critical stresses for the onset and finish of phase transformations and the area of the stress–strain hysteretic loop.

Therefore, this paper aims to develop a constitutive model for SMAs taking into account the isothermal stress cycling degradation, including the accumulation of plastic strain, the evolution of the maximum transformation strain and four transformation temperatures. The new constitutive model is constructed based on the thermodynamic frame proposed by Boyd and Lagoudas [22, 23]. The organization of the paper is as follows: Section 2 presents the observation of cyclic degradation in SMAs through the isothermal stress cycling experiment. The 1-D constitutive model considering the cyclic evolution of the plastic strain, the maximum transformation strain and transformation temperatures is presented in Section 3, while in Section 4, numerical examples are presented and discussed. The conclusions and future work are summarized in the final section.

To simplify the presentation, we denote the two phases related with superelasticity by A and M^d for austenite and detwinned martensite, respectively. The forward and reverse phase transformations are denoted by $A \rightarrow M^d$ and $M^d \rightarrow A$ for austenite to detwinned martensite and detwinned martensite to austenite, respectively.

2. Observation of cyclic degradation

We performed an isothermal stress cycling experiment to a NiTi wire, the wire was repeatedly stressed up to 900 MPa under 28 ^oC. The stress–strain response of the wire is shown in Fig. 1, a simplified diagram which features the evolution of plastic strain, maximum transformation strain and transformation temperatures is shown in Fig. 3, and typical features of cyclic degradation are outlined as follows:

1) The isothermal stress cycling of the NiTi alloy presents an apparent cyclic accumulation of the plastic strain. As shown in Fig. 3(a), after the first cycle, the NiTi wire cannot recover to its original length, and a plastic strain, donated as ε^{p1}, is produced. Similarly, after the second cycle, the total cumulated plastic strain is ε^{p2}, and after the *n*th cycle, the accumulation of the plastic strain becomes ε^{pn}. Furthermore, the plastic strain evolves as an exponential function of cycle number before stabilizing, as shown in Fig. 1 and Fig. 2.

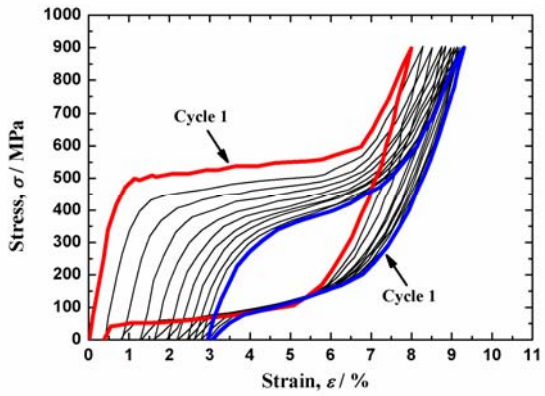

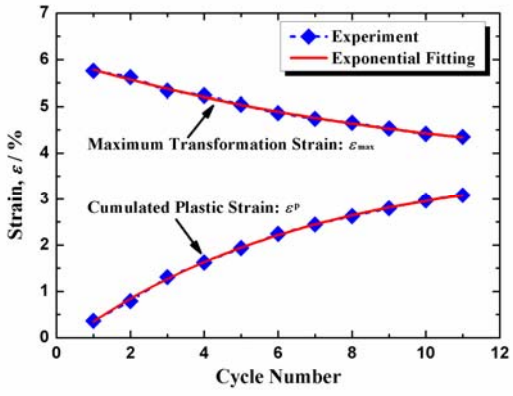

Figure 1. Experimental results of isothermal stress cyclic loading on NiTi wire
Figure 2. Evolution of the maximum transformation strain ε_{max} and plastic strain ε^p during cyclic loading, the experimental results are compared with the exponential fitting results

2) The maximum transformation strain (also referred to as the saturation recovery strain) changes from cycle to cycle. As shown in Fig. 3(a), the maximum transformation strain for cycle 1 is ε_{max1}, while for cycle 2, it reduces to ε_{max2}. Similarly, after the nth cycle, the maximum transformation strain will reduce to ε_{maxn}. Also, as shown in Fig. 2, ε_{max} is found to increase exponentially with respect to the cycle number up to an asymptotic value.

3) The four transformation temperatures change as a function of the cycle number. As shown in Fig. 3 (b), during the first cycle, the four transformation temperatures are M_{s1}, M_{f1}, A_{s1} and A_{f1}, respectively. While in the second cycle, the four temperatures change to M_{s2}, M_{f2}, A_{s2} and A_{f2}. So we can deduce that the four temperatures will change as the cycle number increases. The same phenomenon was reported in literatures [19-21].

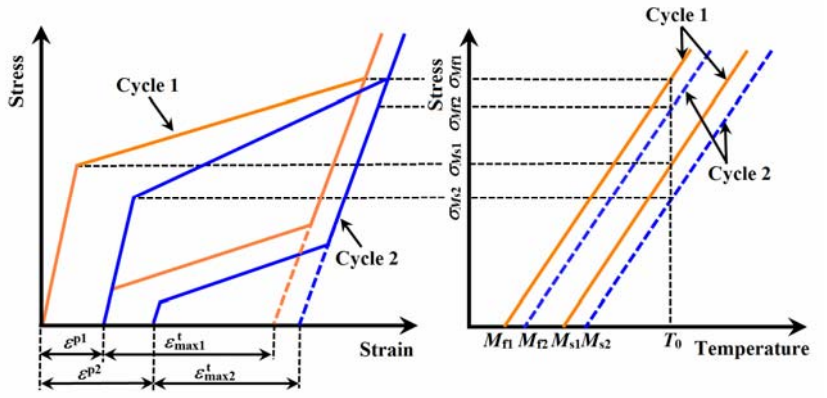

(a) strain evolution (b) transformation temperatures evolution

Figure 3. The evolution of (a): plastic strain, maximum transformation strain in the stress–strain space and (b): transformation temperatures in the stress–temperature space under isothermal stress cycling. For clarity, the evolution of austenite start and finish transformation temperatures is not shown in the stress–temperature space

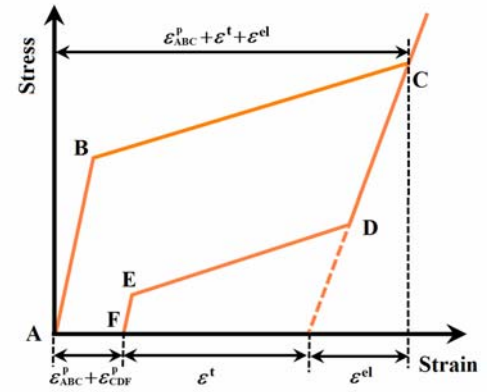

Figure 4. Schematic explanation for the evolution of plastic strain

In order to investigate when the evolution of plastic strain occurs during the whole transformation process, the stress vs. strain response of a typical cycle is presented in Fig. 4. We assume that the plastic and transformation strains produced in A→M^{d} (corresponding loading path is ABC) are separately ε^{p}_{ABC} and ε^{t}, and the elastic strain of point C is ε^{el}. Following these assumptions, the total strain of point C (shown in Fig. 4) becomes:

$$\varepsilon_{C} = \varepsilon^{el} + \varepsilon^{p}_{ABC} + \varepsilon^{t} \tag{1}$$

Assume that the plastic strain for M^{d}→A (corresponding loading path is CDEF) is ε^{p}_{CDF}. Therefore the plastic strain cumulated during the forward and reverse transformations (corresponding loading

path is ACF) is $\varepsilon^{p}_{ABC}+\varepsilon^{p}_{CDF}$. Since the transformation strain can be fully recovered after the $M^{d}\rightarrow A$ transformation, the reduction of the transformation strain during $M^{d}\rightarrow A$ is ε^{t} (corresponding loading path is CDEF, as shown in Fig. 4). Consequently, the total strain of point C can be expressed as:

$$\varepsilon_{D} = \varepsilon^{el} + \varepsilon^{p}_{ABC} + \varepsilon^{p}_{CDF} + \varepsilon^{t} \tag{2}$$

From Eqs. (1) and (2), we can deduce that $\varepsilon^{p}_{CDF}=0$. Following the derivation above, we can assume that the accumulation of plastic strain ε^{p} only occurs during $A\rightarrow M^{d}$.

Consequently, to model the cyclic degradation of shape memory alloys under isothermal stress cycling, the evolution of the plastic strain and maximum transformation strain in $A\rightarrow M^{d}$ and the evolution of transformation temperatures in both forward and reverse transformations must be considered, also related evolution laws should be established.

3. Constitutive model

A constitutive model taking into account the cyclic degradation due to isothermal stress cycling is proposed. It is constructed in the generalized plasticity framework which was employed by Boyd and Lagoudas [22, 23] to simulate the thermo-mechanical behavior of SMA. The construction of the constitutive model is stated in details as follows.

3.1. Strain decomposing and internal variables

3.1.1. Strain decomposing

With the infinitesimal strain assumption, the total strain ε is decomposed into an elastic strain ε^{el} and an inelastic strain ε^{in}:

$$\varepsilon = \varepsilon^{e} + \varepsilon^{in} \tag{3}$$

In which, the inelastic strain ε^{in} can be further decomposed into a thermal expansion strain ε^{th}, a transformation strain ε^{t}, and a plastic strain ε^{p}:

$$\varepsilon^{in} = \varepsilon^{th} + \varepsilon^{t} + \varepsilon^{p} \tag{4}$$

The thermal expansion strain ε^{th} is neglected because the value is much smaller than the others, so the following expression can be got:

$$\varepsilon = \varepsilon^{el} + \varepsilon^{t} + \varepsilon^{p} \tag{5}$$

3.1.2. Internal variables definition

As shown in Eq. (5), two internal variables are needed to account for the evolution of the transformation strain ε^{t} and the plastic strain ε^{p}. Generally, the martensite volume fraction ξ is used as an internal variable to related with ε^{t} [24]:

$$\varepsilon^{t} = \varepsilon_{max}\xi \tag{6}$$

Where ε_{max} is the maximum transformation strain. Following the observation of cyclic degradation stated in Section 2, the plastic strain ε^{p} and the maximum transformation strain ε_{max} change as a function of the cycle number. In order to account for these evolution processes, the cumulated martensite volume fraction ξ^{c} is defined:

$$\xi^{c} = \xi^{ac} + \xi^{mc} \tag{7}$$

Where ξ^{ac} and ξ^{mc} represent the cumulated martensite volume fractions in A→M^{d} and M^{d}→A, respectively. Following these definitions, ξ^{ac} and ξ^{mc} can be expressed as follows:

$$\xi^{ac} = \int \left| \dot{\xi}^{A\to M^{d}} \right| dt,\ \xi^{mc} = \int \left| \dot{\xi}^{M^{d}\to A} \right| dt \tag{8}$$

In which, t is a kinematic time. $\dot{\xi}^{A\to M^{d}}$ and $\dot{\xi}^{M^{d}\to A}$ denote the martensite production rate during A→M^{d} and M^{d}→A.

3.2. Free energy and transformation hardening function

The total Helmoltz free energy ψ for polycrystalline SMAs is given based on Boyd and Lagoudas's work:

$$\psi = E\left(\varepsilon - \varepsilon^{t} - \varepsilon^{p}\right)^{2} \Big/ 2\rho + c\left[\left(T - T_{0}\right) - T\ln\left(T/T_{0}\right)\right] + u_{0} - \eta_{0}T + f(\xi, \dot{\xi}) \tag{9}$$

Where E, c, ρ, η_0 and u_0 are the Young modulus, effective specific heat, mass density, effective specific entropy, and effective specific internal energy at the reference state, respectively. The symbols T and T_0 denote the temperature and reference temperature, respectively. The terms $E(\varepsilon-\varepsilon^{t}-\varepsilon^{p})^{2}/2\rho$, $c[(T-T_0)-T\ln(T/T_0)]$ and $u_0-\eta_0 T+ f(\xi,\dot{\xi})$ represent the elastic strain energy, thermal energy, and the energy related to transformations, respectively.

The effective specific heat c hardly varies during phase transformations, so it is assumed to be constant. However, other material properties in Eq. (9) are assumed to vary with the martensite volume fraction as:

$$E\left(\xi\right) = E^{A} + \xi\left(E^{M} - E^{A}\right) = E^{A} + \xi\Delta E \tag{10}$$

$$\eta_{0}\left(\xi\right) = \eta_{0}{}^{A} + \xi\left(\eta_{0}{}^{M} - \eta_{0}{}^{A}\right) = \eta_{0}{}^{A} + \xi\Delta\eta_{0} \tag{11}$$

$$u_{0}\left(\xi\right) = u_{0}{}^{A} + \xi\left(u_{0}{}^{M} - u_{0}{}^{A}\right) = u_{0}{}^{A} + \xi\Delta u_{0} \tag{12}$$

Where the superscripts A and M represent the austenite and martensite phases, respectively. The symbol Δ denotes the difference of the corresponding material parameter between the martensite and austenite phases.

In particular, the term $f(\xi,\dot{\xi})$ is the transformation hardening function which is used to account for the interactions between the austenite phase and the martensite phase. In this work, a nonlinear transformation hardening model is established:

$$f(\xi,\dot{\xi}) = \left\{a\left[1-\mathrm{sgn}\left(\dot{\xi}\right)\right] + b\left[1+\mathrm{sgn}\left(\dot{\xi}\right)\right]\right\}\left[\left(\frac{\xi}{2}\right)^{2} + \frac{\left(\xi - 1/2\right)^{4}}{2} + \frac{\xi}{4}\right] \tag{13}$$

Where a and b are constitutive model parameters for transformation hardening and they are related to material constants. The function sgn(·) is a signum function of a real number m, it is defined as follow:

$$\mathrm{sgn}(m) = \begin{cases} 1 & \text{if } m > 0 \\ 0 & \text{if } m = 0 \\ -1 & \text{if } m < 0 \end{cases} \tag{14}$$

3.3. Thermodynamic force and constitutive relation

Following the formalism of Truesdell and Noll [25], the Helmoltz free energy ψ and the internal energy u are substituted into the first and second law of thermodynamics to derive thermodynamic constraints on the state of the system resulting in the following constitutive relation:

$$\sigma = \rho \frac{\partial \psi}{\partial \varepsilon} = E\left(\varepsilon - \varepsilon^{\mathrm{t}} - \varepsilon^{\mathrm{p}}\right) \tag{15}$$

Similarly, thermodynamic force X, which is conjugate to the martensite volume fraction ξ, is given:

$$X = -\rho \frac{\partial \psi}{\partial \xi} = -\left[\frac{1}{2}\Delta E\left(\varepsilon - \varepsilon^{\mathrm{t}} - \varepsilon^{\mathrm{p}}\right)^2 - \sigma \frac{d\varepsilon^{\mathrm{t}}}{d\xi} + \rho\left(\Delta u_0 - \Delta \eta_0 T\right) + \frac{df}{d\xi}\right] \tag{16}$$

As assumed in Section 2, the accumulation of plastic strain ε^{p} and the reduction of maximum transformation strain $\varepsilon^{\mathrm{t}}_{\max}$ only occur during A→M$^{\mathrm{d}}$. Therefore, the thermodynamic force Q, which accounts for the evolution of ε^{p} and $\varepsilon^{\mathrm{t}}_{\max}$, is conjugate to the cumulated martensite volume fraction ξ^{ac}. Similar to thermodynamic force X, it can be expressed as:

$$Q = -\rho \frac{\partial \psi}{\partial \xi^{\mathrm{ac}}} = \rho\left(\frac{d\varepsilon^{\mathrm{p}}}{d\xi^{\mathrm{ac}}} + \frac{d\varepsilon^{\mathrm{t}}}{d\xi^{\mathrm{ac}}}\right) \tag{17}$$

3.4. Transformation functions and Kuhn-Tucker inequalities

Borrowed from yield functions in the classical theory of plasticity, transformation functions associated with A→M$^{\mathrm{d}}$ and M$^{\mathrm{d}}$→A are defined as:

$$F^{+} = X + Q - R^{+} \quad \text{when } \dot{\xi} > 0 \quad \text{For the phase transformation: A}\rightarrow\text{M}^{\mathrm{d}} \tag{18}$$

$$F^{-} = -X + Q - R^{-} \quad \text{when } \dot{\xi} < 0 \quad \text{For the phase transformation: M}^{\mathrm{d}}\rightarrow\text{A} \tag{19}$$

Where the constitutive model parameters R^{+} and R^{-} are the radius of the respective transformation domains.

Constraints on the evolution of the martensite volume fraction for the forward and reverse phase transformations are expressed in terms of the Kuhn-Tucker inequalities:

$$\begin{cases} \dot{\xi} \geq 0 \quad F^{+} \leq 0 \quad \dot{\xi} F^{+} = 0 & \text{For the phase transformation: A} \rightarrow \text{M}^{\mathrm{d}} \\ \dot{\xi} \geq 0 \quad F^{-} \leq 0 \quad \dot{\xi} F^{-} = 0 & \text{For the phase transformation: M}^{\mathrm{d}} \rightarrow \text{A} \end{cases} \tag{20}$$

3.5. Evolution laws

Following Eq. (6), the evolution law for the transformation strain ε^{t} can be got:

$$\dot{\varepsilon} = \varepsilon_{\max} \dot{\xi} \tag{21}$$

It is concluded from the experimental results that the material parameter: maximum transformation strain $\varepsilon_{\max}$, varies as an exponential function of the cycle number, as shown in Fig. 2. Furthermore, as explained in Section 3.1.2, $\varepsilon_{\max}$ is assumed to vary only in A→M$^{\mathrm{d}}$, which implies that $\varepsilon_{\max}$ changes as an exponential function of ξ^{ac}. Therefore, from a theoretical point of view, a non-constant material parameter $\varepsilon_{\max}$ can be defined using the evolution law:

$$\dot{\varepsilon}_{\max} = m6\varepsilon^{t}_{\max} e^{-\xi^{ac} m6} \dot{\xi}^{c} \tag{22}$$

Analogous to $\varepsilon_{\max}$, evolution laws of $\varepsilon^{p}_{\max}$ and four material parameters: M_s, M_f, A_s and A_f are given:

$$\dot{\varepsilon}^{p}_{\max} = m5\varepsilon^{p}_{\max} e^{-\xi^{ac} m5} \dot{\xi}^{c} \tag{23}$$

$$M_s = M_{s0} - M_{s\max}\left(1 - e^{-\xi^{c} m1}\right) \tag{24}$$

$$M_f = M_{f0} - M_{f\max}\left(1 - e^{-\xi^{c} m2}\right) \tag{25}$$

$$A_s = A_{s0} - A_{s\max}\left(1 - e^{-\xi^{c} m3}\right) \tag{26}$$

$$A_f = A_{f0} - A_{f\max}\left(1 - e^{-\xi^{c} m4}\right) \tag{27}$$

Where $\varepsilon^{t}_{\max}$, $\varepsilon^{p}_{\max}$, M_{fmax}, M_{smax}, A_{fmax} and A_{smax} denote saturation values of $\varepsilon_{\max}$, ε_p, M_f, M_s, A_f and A_s due to cyclic loading, which can be got through isothermal stress cycling experiments. The variables $m1$~$m6$ can be obtained from the experimental curves by nonlinear fitting method.

So far, the constitutive model of SMAs taking into account the function degradation caused by isothermal stress cyclic loading has been fully established. In the following section, numerical simulations will be performed to verify the proposed model.

4. Simulated results and discussions

To show the model's capability of simulating the macroscopic behaviour of SMA material under isothermal stress cycling, we performed a cyclic tensile test at 5.5% strain amplitude under 27.5 ^{o}C for a SMA wire. Fig. 5 illustrates cyclic stress vs. strain response of the SMA wire for 10 cycles. Numerical simulations are obtained using the constitutive model proposed in this work, and the related material parameters are shown in Table 1. The simulated cyclic stress vs. strain response is shown in Fig. 6. From Fig. 5 and Fig. 6, it may be noticed that the model is able to simulate correctly the main characteristics of the isothermal stress cyclic response of a SMA wire. In particular, the stress vs. strain curves for the 1st, 4th and 10th cycles are shown in Fig. 7 and good agreements between experimental and simulated results are observed.

Table 1. Material parameters used in the constitutive model.

General material parameters	Values	Cyclic material parameters	Values
E^{A}	42200 MPa	M_{smax}	21 K
E^{M}	23500 MPa	M_{fmax}	1.5 K
$\Delta\eta_0$	– 17.77 J /(kg·K)	A_{smax}	0 K
Δu_0	– 20 J /kg	A_{fmax}	0 K
c	4×10^{6} J /(kg·K)	$\varepsilon^{t}_{\max}$	0.0121
ρ	6.5×10^{-9} kg/m^3	$\varepsilon^{p}_{\max}$	0.0141
$A_s(0)$	274K	$m1$	0.14
$A_f(0)$	300 K	$m2$	0.98
$M_s(0)$	270 K	$m3$	0.081
$M_f(0)$	232 K	$m4$	0.05
C_A	9.4 MPa/K	$m5$	0.271
C_M	6.7 MPa/K	$m6$	0.23
$\varepsilon_{\max}(0)$	0.0348		

In order to further investigate the ability of the model to predict the evolution of $\varepsilon_{\max}$, ε^{p} and four

transformation temperatures, the corresponding experimental results are compared with simulated results, as shown in Figs. 8 and 9. It can be seen from these figures that for the evolution of $\varepsilon_{\max}$, ε^{p}, M_s, M_f and A_f, the experimental and simulated results are close to each other. However, for the evolution of A_s, a certain disagreement occurs, which can perhaps be explained that A_s indeed does not evolve exponentially with respect to the cycle number.

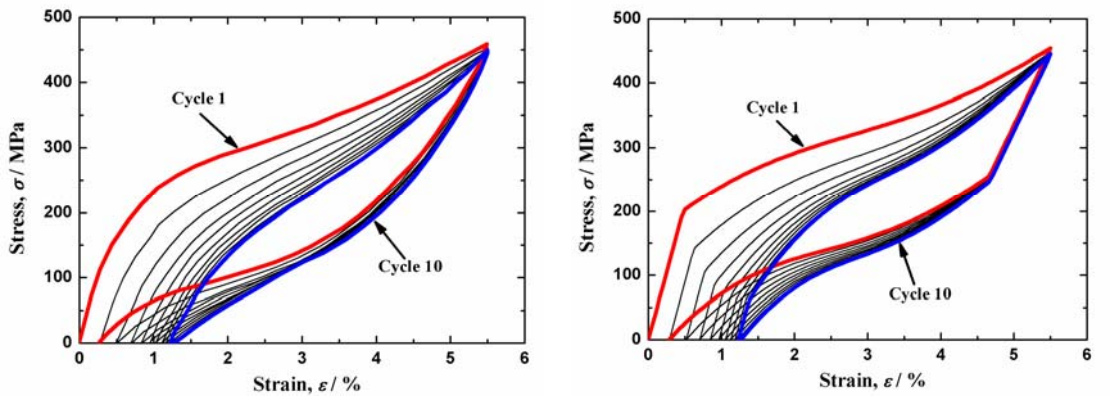

Figure 5. Experimental results of the SMA wire. Isothermal stress cycling at 5.5% strain amplitude under 27.5 ^{o}C for 10 cycles.

Figure 6. Simulated cyclic stress vs. strain curves for 10 cycles using the proposed constitutive model.

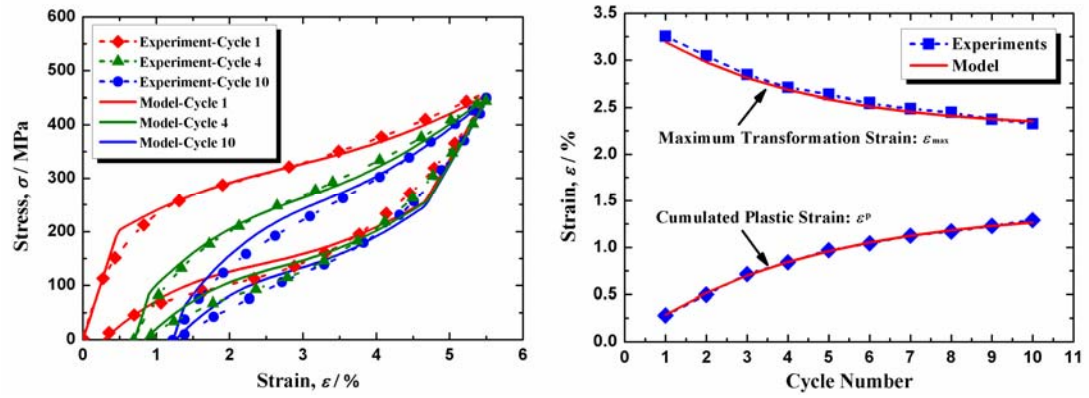

Figure 7. Simulation vs. isothermal stress cyclic loading experimental results for cycle 1, cycle 4 and cycle 10.

Figure8. A comparison of the evolution of plastic strain (ε^{p}) and maximum transformation strain ($\varepsilon_{\max}$) between experimental results and model simulations.

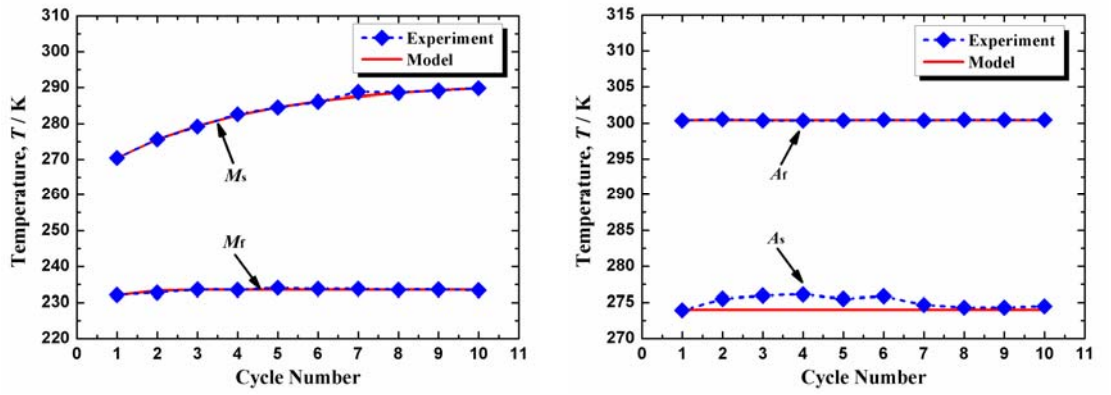

(a) (b)

Figure 9. A comparison of evolution of four transformation temperatures between experimental results and model simulations: (a) M_s and M_f and (b) A_s and A_f.

5. Conclusions and future work

A new 1-D phenomenological model of SMA taking into account the evolution of the plastic strain, maximum transformation strain and transformation temperatures during isothermal stress cycling was introduced in this paper. Since different phase transformation has different influence in the cyclic behaviour, the cumulated martensite volume fraction ξ^{c} was decomposed into ξ^{ac} and ξ^{mc} to account for cyclic effects during corresponding transformation processes. Non-constant material parameters including maximum transformation strain and four transformation temperatures are used. Evolution laws for the non-constant material parameters and plastic strain were established to depict the evolution of maximum transformation strain, transformation temperatures and plastic strain under cyclic loading. Experimental verifications were given and the results showed that the model was able to quantitatively capture the effect of isothermal stress cyclic loading. However, the model cannot simulate the evolution of A_s correctly, which maybe attribute to that A_s actually evolves with a non-experimental function. As a result, future work will introduce a new evolution law for A_s based on experimental studies.

Acknowledgements

The authors are grateful to the financial supported by the National Basic Research Program of China ("973" Project) (Grant No.2010CB631005, 2011CB606105), the National Natural Science Foundation of China (Grant Nos. 90916010, 11172151, 11232008, 11272025) Specialized Research Fund for the Doctoral Program of Higher Education (Grant No.20090002110048), Tsinghua University Initiative Scientific Research Program.

References

[1] K. Otsuka, C.M. Wayman, Shape memory materials, Cambridge Univ Pr, 1999.
[2] N.B. Morgan, Medical shape memory alloy applications - The market and its products. Mater. Sci. Eng. A, 378 (2004) 16-23.
[3] F. Falk, Model free energy, mechanics and thermodynamics of shape memory alloys. Acta Metall., 28 (1980) 1773-1780.
[4] K. Tanaka, Thermomechanical sketch of shape memory effect: one-dimensional tensile behavior. Res. Mech., 18 (1986) 251-263.
[5] Q.P. Sun, K.C. Hwang, Micromechanics modelling for the constitutive behavior of polycrystalline shape memory alloys. II. Study of the individual phenomena. J. Mech. Phys. Solids, 41 (1993) 19-33.
[6] Q.P. Sun, K.C. Hwang, Micromechanics modelling for the constitutive behavior of polycrystalline shape memory alloys. I. Derivation of general relations. J. Mech. Phys. Solids, 41 (1993) 1-17.
[7] D.C. Lagoudas, Z. Bo, M.A. Qidwai, Unified thermodynamic constitutive model for SMA and finite element analysis of active metal matrix composites. Mech. Compos. Mate.r Struct., 3 (1996) 153-179.
[8] F. Auricchio, R.L. Taylor, Shape-memory alloys: Modelling and numerical simulations of the finite-strain superelastic behavior. Comput. Methods Appl. Mech. Eng., 143 (1997) 175-194.
[9] X.W. Du, G. Sun, S.S. Sun, Piecewise linear constitutive relation for pseudo-elasticity of shape memory alloy (SMA). Mater. Sci. Eng. A, 393 (2005) 332-337.
[10] S. Reese, D. Christ, Finite deformation pseudo-elasticity of shape memory alloys -

Constitutive modelling and finite element implementation. Int. J. Plast., 24 (2008) 455-482.

[11] C. Lexcellent, G. Bourbon, Thermodynamical model of cyclic behaviour of Ti-Ni and Cu-Zn-Al shape memory alloys under isothermal undulated tensile tests. Mech. Mater., 24 (1996) 59-73.

[12] R. Abeyaratne, S.J. Kim, Cyclic effects in shape-memory alloys: A one-dimensional continuum model. Int. J. Solids Struct., 34 (1997) 3273-3289.

[13] F. Auricchio, E. Sacco, Thermo-mechanical modelling of a superelastic shape-memory wire under cyclic stretching-bending loadings. Int. J. Solids Struct., 38 (2001) 6123-6145.

[14] K. Tanaka, F. Nishimura, T. Hayashi, H. Tobushi, C. Lexcellent, Phenomenological analysis on subloops and cyclic behavior in shape memory alloys under mechanical and/or thermal loads. Mech. Mater., 19 (1995) 281-292.

[15]X. Feng, Q. Sun, Shakedown analysis of shape memory alloy structures. Int. J. Plast., 23 (2007) 183-206.

[16] Q. Kan, G. Kang, Constitutive model for uniaxial transformation ratchetting of super-elastic NiTi shape memory alloy at room temperature. Int. J. Plast., 26 (2010) 441-465.

[17] W. Zaki, Z. Moumni, A 3D model of the cyclic thermomechanical behavior of shape memory alloys. J. Mech. Phys. Solids, 55 (2007) 2427-2454.

[18] L. Saint-Sulpice, S. Arbab-Chirani, S. Calloch, Thermomechanical cyclic behavior modeling of Cu-Al-Be SMA materials and structures. Int. J. Solids Struct., 49 (2012) 1088-1102.

[19] M.F.X. Wagner, S.R. Dey, H. Gugel, J. Frenzel, C. Somsen, G. Eggeler, Effect of low-temperature precipitation on the transformation characteristics of Ni-rich NiTi shape memory alloys during thermal cycling. Intermet., 18 (2010) 1172-1179.

[20] Q. Hu, W. Jin, X.P. Liu, M.Z. Cao, S.X. Li, The transformation behavior and the shape memory effect due to cyclic stress/strain for Ti-49.6Ni alloy. Mater. Lett., 54 (2002) 114-119.

[21] D.A. Hebda, S.R. White, Effect of training conditions and extended thermal cycling on nitinol two-way shape memory behavior. Smart Mater. Struct., 4 (1995) 298-304.

[22] J. Boyd, A thermodynamical constitutive model for shape memory materials. Part I. The monolithic shape memory alloy. Int. J. Plast., 12 (1996) 805-842.

[23] J. Boyd, A thermodynamical constitutive model for shape memory materials. Part II. The SMA composite material. Int. J. Plast., 12 (1996) 843-873.

[24] P. Vacher, C. Lexcellent, Study of pseudoelastic behaviour of polycrystalline shape memory alloys by resistivity measurements and acoustic emission. Proceedings of the 6th International Conference on Mechanical Behaviour of Materials, 07/29 - 08/ - 2/91 (Kyoto, Jpn, 1992).

[25] C. Truesdell, W. Noll, S.S. Antman, The non-linear field theories of mechanics, Springer Verlag, 2004.